MS003

Developing a modelling tool for hydrothermal deposition of Yttrium-Stabilized Zirconia (YSZ) thin films

Medha Shridharan

Report

I. Introduction

Yttrium-stabilized Zirconia (YSZ) is a ceramic material in which the crystal structure of ZrO_2 is stabilized by doping with Y_2O_3, as illustrated in Figure 1. [1]

It has various unique and desirable properties, including low thermal conductivity and the ability to act as a solid electrolyte. Due to these properties, these thin films are currently used in a myriad of applications, including in solid-oxide fuel cells and in thermal-barrier coatings (TBC) for wind turbines. [2] More exceptionally, YSZ thin films are currently being developed for countless novel and promising applications. From *Dykas et al. (2019*), we observe the various positive effects YSZ has on cell adherance and proliferation. For instance, figure 2 illustrates the increase in differentiated adipocytes with lipid formation which was observed on the (b) Y_2O_3 - ZrO_2 coated substrate as opposed to (a) the control substrate. Hence, YSZ is a highly promising material in upcoming fields, such as cell-culture meat, and is also useful in medical implants.[3]

There are several ways of synthesizing YSZ thin films, including pulsed laser deposition (PLD), sol-gel and hydrothermal synthesis. [4]

Hydrothermal synthesis is an especially highly attractive chemical process to directly prepare submicrometer- and nanometer-sized polycrystalline metal oxides as it is rapid, energy-efficient, allows for easy waste-processing, is suitable for large-scale processing and has minimal environmental impact. [5-8] In the case of growing YSZ thin films for cell-culture meat and medical implant applications, hydrothermally synthesised thin films also adhere better to the substrate as compared to those synthesised by other methods, hence minimising flaking of the film and preventing YSZ contamination in the cultured cells.

From *Tsukada et al. (2014)*, the hydrothermal synthesis of YSZ thin films is conducted by placing an aqueous solution of yttrium nitrate ($Y(NO_3)_3$), zirconyl chloride ($ZrOCl_2$) and potassium hydroxide (KOH) in an autoclave, following which YSZ deposits out of the solution onto a substrate to form a thin film (illustrated in Figure 3).

It has been found that that the surface morphology of the synthesized YSZ thin film depends on its rate of deposition and solubility in the solution, which in turn depends on the

pH of the solution mixture. Naturally, the pH of the reagent solution depends on the concentrations of $Y(NO_3)_3$, $ZrOCl_2$ and KOH added to the solution mixture.

Hence, a researcher who wants to manufacture YSZ of a desired surface morphology for a new application needs to determine the set of reagent concentrations and by extension, solubilities required for the task. However, currently, no such model exists to predict YSZ solubility as the chemical equilibrium equations needed for these calculations are not readily available. Hence, extensive trial-and-error studies are required to determine these concentrations. This slows down research timelines, results in the excessive wastage of resources and increases the environmental impacts of synthesis.

II. Engineering objective of model

The objective of this research is to develop an equilibrium modelling tool with an interactive dashboard to help researchers narrow down the set of reagent concentrations which could generate a YSZ thin film of their desired surface morphology.

Our dashboard displays a grid of $[Y(NO_3)_3]$,$[ZrOCl_2]$ tuples, with the input [KOH] adjusted by a slider. The dashboard also displays scanning electron microscope (SEM) or transmitting electron microscope (TEM) images of YSZ films obtained from empirical literature, which researchers can then use to determine the image closest to their desired surface morphology. Researchers can then utilize the pH and solubility contour lines in the grid to identify the pH and solubility bands in which their desired morphology is likely to lie.

III. Methodology

Python 3.9.6 was used for all modelling with sympy 1.8, numpy 1.21.1 and matplotlib 3.4.2 were used to generate data and plot the results. Pycharm Community Edition 2021.2.3 was used to write the model on the Windows operating system in an Anaconda 4.10.3 virtual environment. All programs were written in python.

Phase 1: Computing solubility and pH values to draw contour lines

We first collected the equilibrium constants for speciation from various sources and verified them against each other.

Tsukuda et al. (2014) provided the quotients of reaction for the relevant reactions in the yttrium and zirconium system. Using these, the equilibrium concentrations of each species were determined using stoichiometry from the chemical reaction. An example equation for how this was determined is shown below.

$$A + 2B \Leftrightarrow 3C + D$$

	A	B	C	D
Initial	1	1	0	0
Change	-a	-2a	+3a	+a
Equilibrium	1-a	1-2a	+3a	+a

$$K_{rxn} = \frac{[3a]^3[a]}{[1-a][1-2a]^2}$$

The pH of the solution depends on [OH-] from the dissociation of KOH in aqueous medium. However, it cannot be assumed that all OH- ions from KOH remain free in solution. Some OH- ions react to form species of Y and Zr in solution and are effectively "locked" in these compounds. The chemical equilibrium equations for their formation are as follows:

Speciation reactions for Zr	$\log Q_{x,y}^*$	
$Zr^{4+} + H_2O \Leftrightarrow Zr(OH)^{3+}_{(aq)} + H^+$	0.3	(1.1)
$Zr^{4+} + 2H_2O \Leftrightarrow Zr(OH)_2{}^{2+}_{(aq)} + 2H^+$	-1.70	(1.2)
$Zr^{4+} + 3H_2O \Leftrightarrow Zr(OH)_3{}^{+}_{(aq)} + 3H^+$	-5.10	(1.3)
$Zr^{4+} + 4H_2O \Leftrightarrow Zr(OH)_{4(aq)} + 4H^+$	-9.70	(1.4)
$Zr^{4+} + 5H_2O \Leftrightarrow Zr(OH)_5{}^{-}_{(aq)} + 5H^+$	-16.00	(1.5)
$3Zr^{4+} + 4H_2O \Leftrightarrow Zr_3(OH)_4{}^{8+}_{(aq)} + 4H^+$	-0.6	(1.6)
$3Zr^{4+} + 5H_2O \Leftrightarrow Zr_3(OH)_5{}^{7+}_{(aq)} + 5H^+$	-3.70	(1.7)
$4Zr^{4+} + 8H_2O \Leftrightarrow Zr_4(OH)_8{}^{8+}_{(aq)} + 8H^+$	6.0	(1.8)

Speciation reactions for Y	$\log Q_{x,y}^*$	
$Y^{3+}_{(aq)} + H_2O \Leftrightarrow Y(OH)^{2+}_{(aq)} + H^+$	-7.7	(2.1)
$Y^{3+}_{(aq)} + 4H_2O \Leftrightarrow Y(OH)_4{}^{-}_{(aq)} + 4H^+$	-36.5	(2.2)

$2Y^{3+}_{(aq)} + 2H_2O \Leftrightarrow Y_2(OH)_2^{4+}{}_{(aq)} + 2H^+$	-14.23	(2.3)
$3Y^{3+}_{(aq)} + 5H_2O \Leftrightarrow Y_3(OH)_5^{4+}{}_{(aq)} + 5H^+$	-31.6	(2.4)
$Y^{3+}_{(aq)} + 3H_2O \Leftrightarrow Y(OH)_{3(s)} + 3H^+$	-17.5	(2.5)
$Y(OH)_{3(s)} \Leftrightarrow Y(OH)_{3(aq)}$	-8.5	(2.6)

*For the metal hydrolysis reaction given by $xM^{z+}(aq) + yH_2O \Leftrightarrow M_x(OH)_y{}^{(zx-y)+}(aq) + yH^+$, and the corresponding mass-action equation defined by $Q_{x,y} = [M_x(OH)_y{}^{(zx-y)+}][H^+]^y/[M^{z+}]^x$.

These equations can be generalised into the following forms for Zr and Y respectively:

$$nZr^{4+} + mH_2O \rightleftharpoons Zr_n(OH)_m^{x(+/-)} + mH^+ \quad (3.1)$$

$$aY3+ + bH2O \rightleftharpoons Y_a(OH)_b{}^{y(+/-)} + bH^+ \quad (3.2)$$

In our model, we leverage these chemical equilibrium equations to account for the formation of these species. We then derived simultaneous equations from these chemical equilibria and used them to compute the precise concentration of OH- ions in the solution. This allows us to find the pH of the solution mixture.

Although theoretically either $[H^+]$ or $[OH^-]$ in solution can be used to determine pH of a solution, researchers have control over [KOH] added to the solution and hence, this concentration is used as an upper bound for the concentration of free OH- ions in solution. In contrast, $[H^+]$ cannot be bounded so easily and hence, $[OH^-]$ is chosen for the calculation of pH for each [KOH].

Once pH for various sets of reagent concentrations could be determined, the solubility of Y and Zr over a pH range was determined. As solubility affects the rate of deposition and subsequently the surface morphology of the synthesised YSZ film, the variation of solubility over various pH values was a key point to identify.

In this step, various [KOH] values were iterated between 0.001M and 5M were iterated and the solubilities of Y and Zr were found. In this step, we compute the solubilities of Yt and Zr in the solution by summing up the concentrations of all Y-based and Zr-based species formed in the solution respectively, as represented by the following equation:

$$\text{Solubility} = \sum [M_x(OH)_y{}^{(zx-y)+}], \text{ where M refers to Y or Zr} \quad (4)$$

These solubility values vary significantly with pH. They were initially plotted for pure $Y(NO_3)_3$ + KOH and $ZrOCl_2$ + KOH systems, as shown in Figures 4 and 5 respectively.

Finally, Figure 6 illustrates the change in solubilities for Yttrium and Zirconium species together in a single solution.

This was done by iterating through various values of KOH and identifying the point at which the net charge of the solution is zero via the toms748 algorithm in the optimize package. This root-finding algorithm combines techniques from the bisection method and Newton-rhapson method to rapidly find the root of any given equation.

Creating visualizations of the contour lines for the dashboard followed from these Phase 1 computations. These contour lines were plotted on Streamlit 1.3.0 on a solubility surface plot, displayed as a grid of [$Y(NO_3)_3$] and [$ZrOCl_2$] values on the y- and x-axes respectively. A slider for [KOH] was added to the interactive Streamlit dashboard such that the [KOH] added could be adjusted with ease.

Phase 2: Adding SEM/TEM images from empirical literature

In phase 2, we leverage existing empirical literature to append a selection of Scanning Electron Microscope (SEM) or Transmitting Electron Microscope (TEM) images of YSZ surfaces to the grid, each at the set of reagent concentrations it was synthesized under.

For instance, we consider the synthesis conducted by *Zarkov et al. (2015)*. Coprecipitation was conducted with $Zr(CH_3COO)_x$, $Y(CH_3COO)_y$, $C_2H_2O_4$ and NH_4OH at 50ºC at pH 9-10 for 0.5h. It was then annealed at 1500ºC for 5h and an SEM was taken of the final product, 8mol% YSZ powder (shown below in figure 7).

Based on these synthesis conditions, the image is added to the corresponding point on the solubility surface plot in the Streamlit dashboard to allow researchers to visualise the surface morphology of a thin film grown at the particular set of reagent concentrations.

IV. Results & Discussions

The final solubility surface plots for YSZ are obtained via this model and displayed on the interactive Streamlit dashboard. The solubility surface plot is displayed as a grid, with the y- and x-axes corresponding to [$Y(NO_3)_3$] and [$ZrOCl_2$] respectively. Hence, the coordinates of each point on the grid represents a tuple of the concentrations of $Y(NO_3)_3$ and $ZrOCl_2$ added to the solution mixture.

The solubilities of Y and Zr, and hence the solubility surface plot, changes as the concentration of KOH added to the solution varies due to the changes in the amount of Y and Zr species formed. Figure 8 below shows the interactive dhasboard at two different input [KOH]. (a) shows the solubilities when KOH = 0.1M while (b) shows the plot when KOH=0.5M. Hence, as expected, the pH values in (b) are much higher than those in (a). [KOH] is adjusted by a slider on the dashboard.

From this, we can see that our model is highly effective in adjusting for these changes and can account for the complexity of the solution mixture system.

There is a restriction on the range of values the equations work for. Beyond [KOH]=0.5M at high pH, new species are formed in solution, and hence a new set of equations will be needed to define the solutions at this concentration. The model does not work beyond this value.

Figure 9 illustrates the final output of the dashboard. The red lines represent pH. The points with concentration tuples as their coordinates yield a given pH value. The blue lines represent the solubility of yttrium species while the green lines represent solubility of zirconium species Along these lines, the concentration tuples yield a given solubility.
In these grids, the SEM images of surface morphologies from empirical data are obtained and mapped at the corresponding concentration tuple on the grid. This allows for easy visualisation of the various sets of reagent concentrations which can be used to grow specific thin films of YSZ.

For example, figure 10 illustrates the solubility surface plot for YSZ at KOH = 0.5M. The SEM image of Zarkov's synthesis (from figure 8) is an example of a surface morphology which a researcher might desire for their application. Suppose the researcher scrolls over the grid and identifies this SEM image as the surface morphology closest to their desired morphology. They can then narrow the set of reagent concentrations they test to those within the pH bands 9 and 10. In other words, they can narrow the range of concentrations they test as they know the solution mixture required to produce their desired YSZ thin film output must have a pH of between 9 and 10.

V. Conclusions & Future work

In conclusion, this model helps researchers to generate useful insights into the growth mechanics of YSZ, allowing them to hone their growth strategy for their desired output to be used in the wide array of applications stated above, making it highly effective in minimizing the need for trial-and-error studies. This helps to greatly speed up research timelines, minimize the wastage of resources and minimize the environmental impacts of synthesis.

The next step for this model will be to add temperature dependence of the solubility equilibrium constants of YSZ to this model. This is an especially useful feature as in hydrothermal synthesis, most synthesis is conducted at a temperature above 100ºC. Beyond this temperature, the water in the autoclave reaches its boiling point and the pressure in the vessel increases, resulting in changes in solubilities of yttria and zirconia.

VI. Bibliography & References

[1] Tsampas, M. N., Sapountzi, F. M., & Vernoux, P. (2015). Applications of yttria stabilized zirconia (YSZ) in catalysis. Catalysis Science & Technology, 5(11), 4884–4900. doi:10.1039/c5cy00739a

[2] Tsukada, T., Venigalla, S., Morrone, A. A., & Adair, J. H. (2004). Low-Temperature Hydrothermal Synthesis of Yttrium-Doped Zirconia Powders. Journal of the American Ceramic Society, 82(5), 1169–1174. doi:10.1111/j.1151-2916.1999.tb01891.x

[3] Dykas, M. M. et al. (2019, November 14). Thin Film Deposited Inorganic Metal Oxide As A Selective Substrate For Mammalian Cell Culture And As An Implant Coating.

[4] Jilani, A., Abdel-wahab, M. S., & HosnyHammad, A. (2017, March 8). Advance deposition techniques for thin film and coating. IntechOpen. Retrieved January 15, 2022, from https://www.intechopen.com/chapters/52684

[5] A. R. Burkin, H. Saricimen, and B. C. H. Steele, “Preparation of Yttria Stabilized Zirconia Powders by High Temperature Hydrolysis,” Trans. J. Br. Ceram. Soc., **79**, 105 (1980).

[6] E. P. Stambaugh, J. H. Adair, I. Sekercioglu, and R. R. Wills, “Hydrothermal Method for Producing Stabilized Zirconia,” U.S. Pat. No. 4 619 817, Oct. 28, 1986.

[7] K. Hishinuma, T. Kumaki, Z. Nakai, M. Yoshimura, and S. Somiya, “Characterization of Y2O3–ZrO2 Powder Synthesized under Hydrothermal Conditions”; p. 201 in Advances in Ceramics, Vol. 24, Science and Technology of Zirconia III. Edited by S. So¯miya, N. Yamamoto, and H. Yanagidas. American Ceramic Society, Westerville, OH, 1986.

[8] W. Kriechbaum, P. Kleinschmit, and D. Peuckert, “Wet Chemical Synthesis of Zirconia Powders”; p. 146 in Ceramic Transactions, Vol. 1, Ceramic Powder Science II A. Edited by G. L. Messing, E. R. Fuller Jr., and H. J. Hausner. American Ceramic Society, Westerville, OH, 1988

VII. Appendix

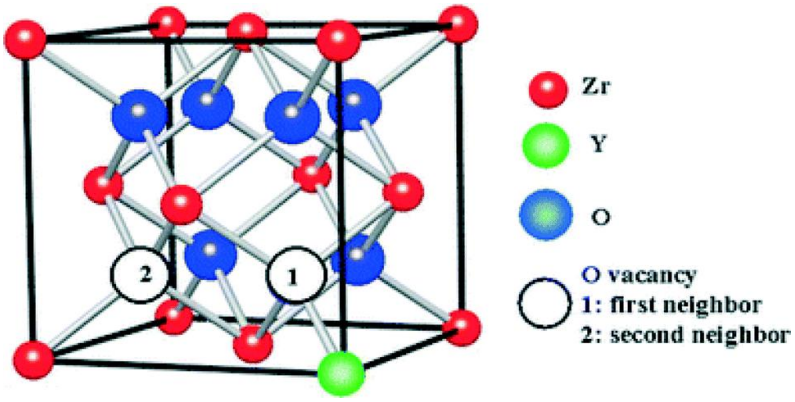

Figure 1: Structure of YSZ [1]

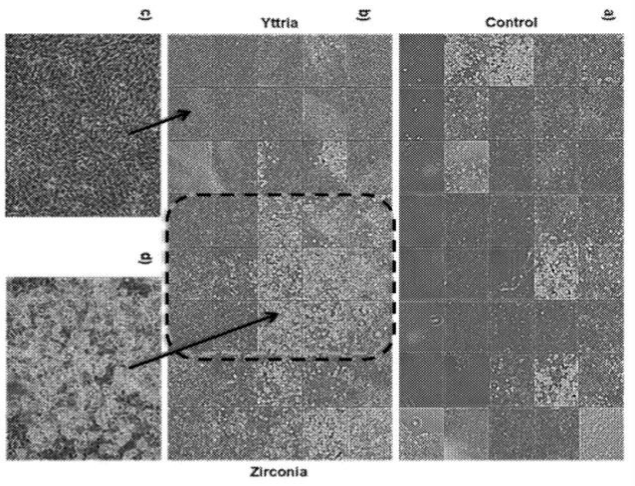

Figure 2: An increase in differentiated adipocytes with lipid formation was observed on the (b) Y_2O_3 - ZrO_2 coated substrate as opposed to (a) the control substrate[3]

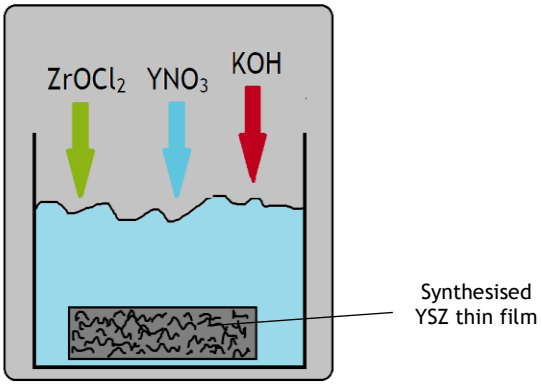

Figure 3: Illustration of the hydrothermal synthesis of YSZ in an autoclave

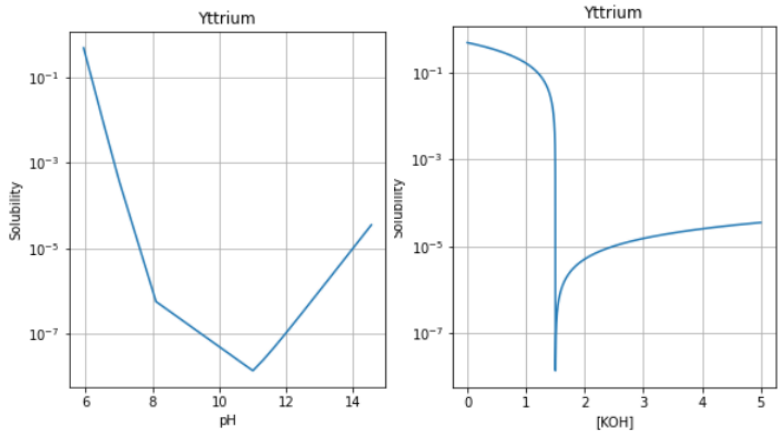

Figure 4: Solubility of Yttrium plotted against pH and [KOH]/M in $Y(NO_3)_3$ + KOH system

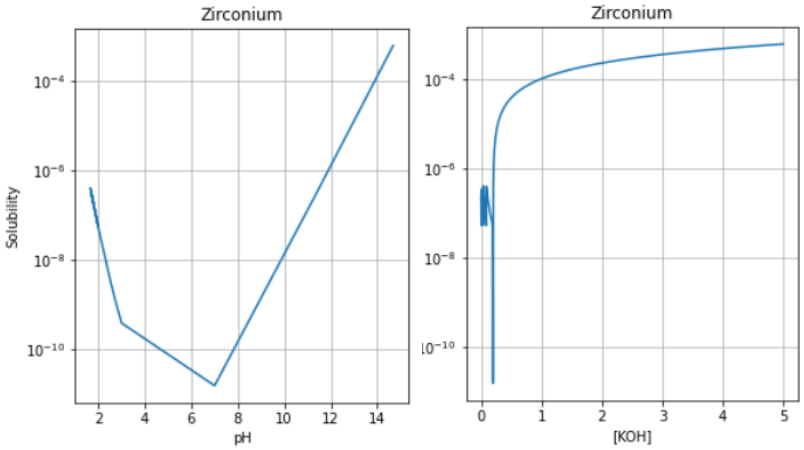

Figure 5: Solubility of Zirconium plotted against pH and [KOH/M in $ZrOCl_2$ + KOH system

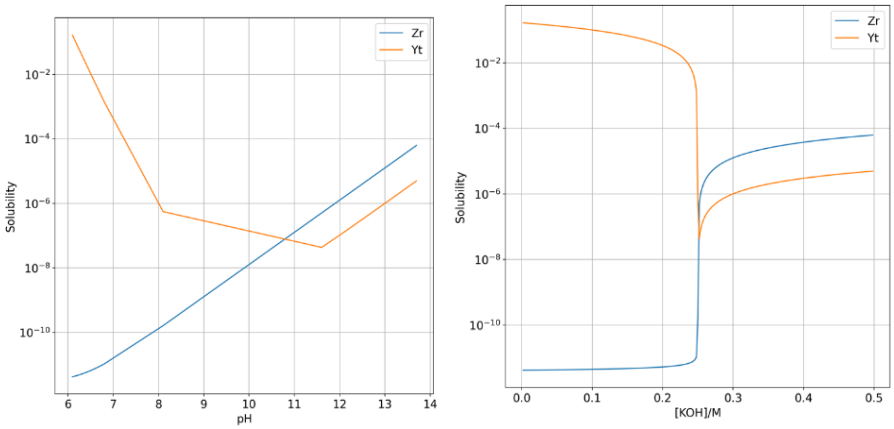

Figure 6: The change in solubilities of Yttrium and Zirconium species in $Y(NO_3)_3$+$ZrOCl_2$+KOH

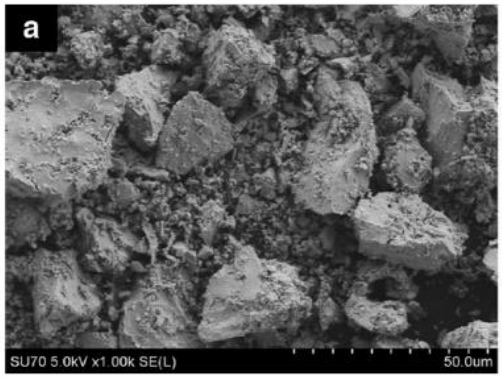

Figure 7: SEM Micrograph of 8mol% YSZ powder synthesised by coprecipitation at pH 9-10 (Zarkov et al, 2015)

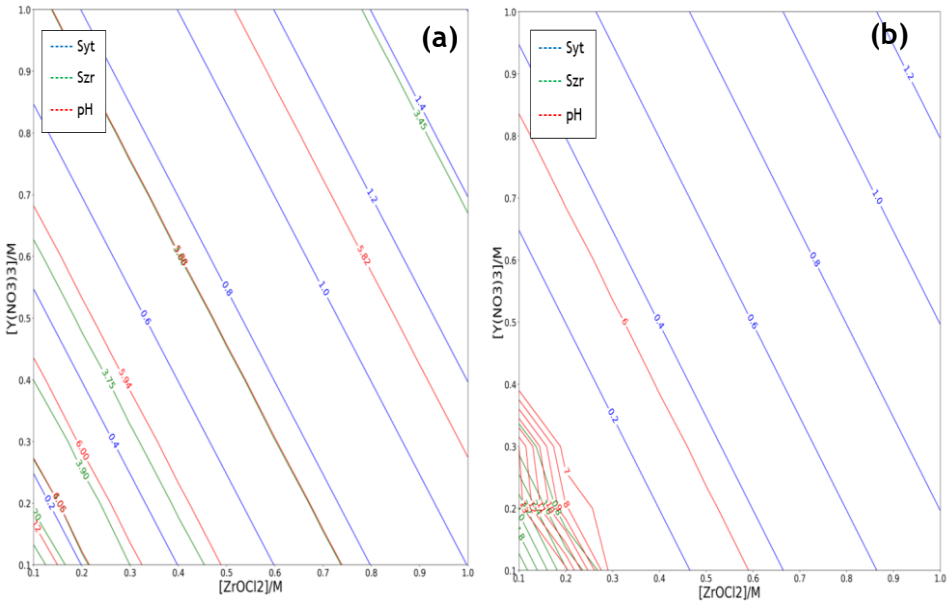

Figure 8: Solubility surface plot for YSZ. Each point is a tuple of ([Zr], [Y]) for (a) [KOH] = 0.1M and (b) [KOH] = 0.5M. [KOH] is adjusted by slider on dashboard, given [KOH]≤0.5M.

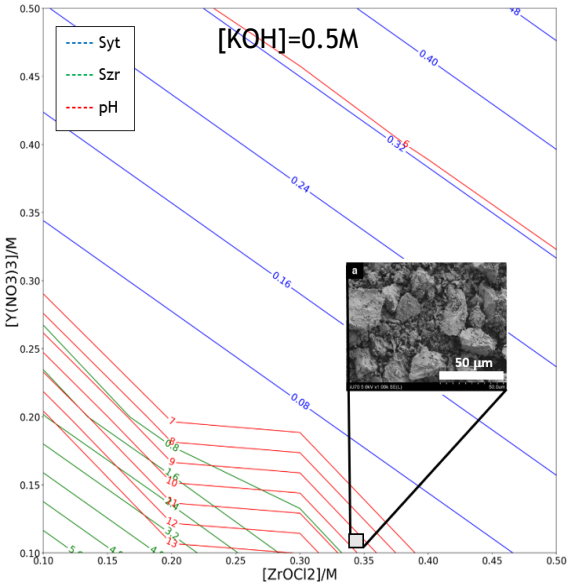

Figure 9: Solubility surface plot for YSZ with SEM Micrograph of 8mol% YSZ powder synthesised by coprecipitation at pH 9-10 (Zarkov et al, 2015)